PEDS Advance Access published February 13, 2009

Protein Engineering, Design & Selection pp. 1–7, 2009
doi:10.1093/protein/gzp004

The C-terminal domain of the HIV-1 Vif protein is natively unfolded in its unbound state

Tali H. Reingewertz[1], Hadar Benyamini[1], Mario Lebendiker[2], Deborah E. Shalev[2] and Assaf Friedler[1,3]

[1]Institute of Chemistry and [2]The Wolfson Centre for Applied Structural Biology, Hebrew University of Jerusalem, Safra Campus, Givat Ram, 91904 Jerusalem, Israel

[3]To whom correspondence should be addressed.
E-mail: assaf@chem.ch.huji.ac.il

The human immunodeficiency virus type-1 (HIV-1) Vif protein neutralizes the cellular defense mechanism against the virus. The C-terminal domain of Vif (CTD, residues 141–192) mediates many of its interactions. Full-length Vif is difficult to purify in large amounts, hence the only available structure of Vif is of residues 140–155 within the ElonginBC complex. Other structural information, derived from modeling and indirect experiments, indicates that the Vif CTD may be unstructured. Here, we chemically synthesized the Vif CTD using pseudo-proline-building blocks, studied its solution structure in the unbound state using biophysical techniques and found that it is unstructured under physiological conditions. The circular dichroism (CD) spectrum of Vif CTD showed a pattern of random coil with residual helical structure. The ^{15}N-HSQC nuclear magnetic resonance (NMR) spectrum was characteristic of natively unfolded peptides. Vif CTD eluted from an analytical gel filtration column earlier than expected, indicating an extended conformation. Disorder predictions found the CTD to be unstructured, in agreement with our experimental results. CD experiments showed that Vif CTD underwent a conformational change upon interacting with membrane-mimicking DPC micelles, but not upon binding to a peptide derived from its binding region in ElonginC. Our results provide direct evidence for the unfolded structure of the free Vif CTD and indicate that it may gain structure upon binding its natural ligands.

Keywords: biophysics/HIV-1/natively unfolded proteins/peptides/Vif

Introduction

Natively unfolded or intrinsically disordered proteins and protein domains are characterized by an almost complete lack of secondary and tertiary structure and an extended conformation with high flexibility (Uversky *et al*., 2000; Dunker *et al*., 2001; Tompa, 2002; Fink, 2005). Natively unfolded regions usually mediate binding to numerous partner ligands, which may be followed by the induction of a structure that is required for the specific interaction (Dyson and Wright, 2005; Tompa, 2005; Wright and Dyson, 1999).

The human immunodeficiency virus type-1 (HIV-1) accessory protein, viral infectivity factor (Vif), is a 23 kDa protein of 192 amino acids (Sodroski *et al*., 1986). HIV-1 infection, in many target cells, requires Vif in order to produce infectious progenies (Strebel *et al*., 1987; Borman *et al*., 1995). Vif acts by neutralizing the cellular mechanism of anti-HIV defense by interacting with the cellular cytosine deaminase APOBEC-3G (A3G) and neutralizing its anti-viral activity (Mariani *et al*., 2003; Yu *et al*., 2003). Vif targets A3G for degradation in the ubiquitin-proteasome pathway by forming an E3 ubiquitin ligase complex. Vif is located both in the soluble and membrane-bound fractions of the cytoplasm of infected cells (Goncalves *et al*., 1995).

Vif consists of several functional domains (Fig. 1A). These include the RNA-binding domain and a binding region for A3G at the N-terminus, a central domain that is involved in interactions with A3G and the viral protease, a His-Cys-Cys-His- zinc binding motif and Cul5 binding region, and a C-terminal domain (CTD) that mediates the interactions of Vif with the HIV-1 Gag protein (Bouyac *et al*., 1997; Simon *et al*., 1997), the cellular protein ElonginC (Mehle *et al*., 2004) and the host cell membrane (Lake *et al*., 2003). Vif CTD binds ElonginC through a SOCS box domain (Mehle *et al*., 2004; Cao *et al*., 2005), containing a BC-box at amino acids 144–159, and a cullin-box at amino acids 159–173 (Stanley *et al*., 2008) as part of the E3 ubiquitin ligase complex that sends A3G to degradation. The Vif CTD is tightly associated with the cytoplasmic side of the host cell membranes through AA 172–192 (Goncalves *et al*., 1994, 1995). Residues 151–164 in the CTD have been shown to mediate oligomerization of Vif (Yang *et al*., 2001, 2003). Vif is processed by the viral protease in the CTD, releasing the segment 151–192 (Khan *et al*., 2002). This process is important for the function of Vif, since impairing the ability of the viral protease to process Vif, impairs Vif function. The CTD of Vif is important for the viability of the virus since it mediates many of the interactions of Vif with its partner molecules.

The only available crystal structure of a Vif domain was solved recently: The structure of a peptide derived from the Vif SOCS box (residues 139–176) in complex with ElonginBC, as a part of the E3 ubiquitin ligase complex (Stanley *et al*., 2008). The structure shows that residues 140–155 of Vif (the BC-box) adopt a helix–loop conformation when bound to the ElonginBC complex. Electron density was not observed for other regions of the Vif 139–176 fragment, probably due to disorder.

There remains a lack of structural and quantitative biophysical information at the molecular level of Vif, particularly in its unbound state. This is partly due to the difficulty in expressing and purifying Vif in the amounts required for high-resolution structural and biophysical studies. Structural information on the free Vif protein has been derived from theoretical predictions and indirect experiments (Barraud *et al*., 2008). Two homology models that predicted the overall tertiary structure of Vif differed significantly from each other: One predicted the CTD of Vif to be unfolded (Balaji *et al*., 2006) (PDB code: 1VZF), while this region was not included in the other (Lv *et al*., 2007). Disorder prediction servers also predicted that the Vif CTD is unstructured (Auclair *et al*., 2007; Barraud *et al*., 2008). Indirect

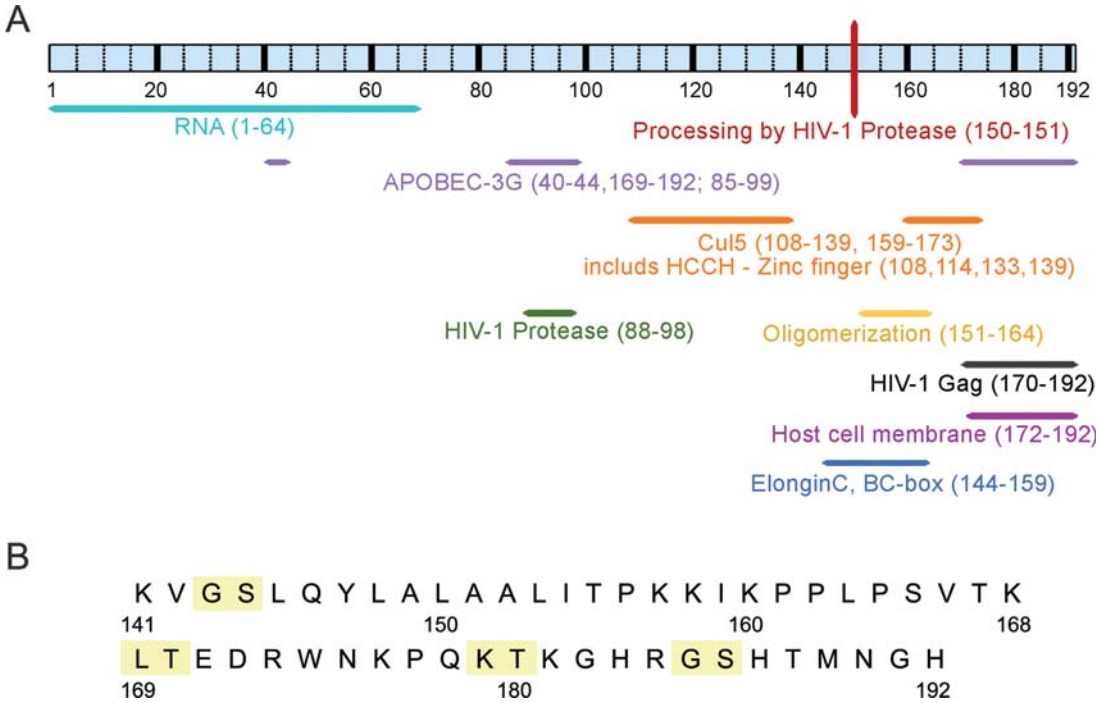

Fig. 1. Schematic representation of Vif sequence and interactions: (**A**) interactions between Vif and its partners with an indication of the binding region in Vif. (**B**) Location of the pseudoproline dipeptides in the chemically synthesized Vif CTD.

experiments using chemical cross-linking, proteolysis and mass spectrometry analysis showed that the CTD of Vif was intrinsically disordered and became ordered upon oligomerization (Auclair *et al*., 2007).

Here, we provide direct evidence for the unstructured nature of the unbound Vif CTD. This region was synthesized and its structure and interactions were analyzed using biophysical methods including circular dichroism (CD), analytical gel filtration, NMR and fluorescence spectroscopy. Vif CTD exhibited properties typical of a natively unfolded region under physiological conditions, giving a random coil with residual α-helix or poly (L-proline) type II helix (ppII). Vif CTD underwent a structural change when dissolved in DPC micelles that were used to model the interaction with the cell membrane, but not upon binding to a peptide derived from its binding region in ElonginC. This indicates that the Vif CTD may increase its structural content upon binding its natural ligands.

Materials and methods

Peptide synthesis, labeling and purification

Peptides were synthesized using standard SPPS methods on an Applied Biosystems (ABI) 433A peptide synthesizer using Fmoc chemistry and labeling as described (Hayouka *et al*., 2007). The peptide derived from ElonginC 76–111 was labeled using 5′ and 6′ carboxyfluorescein succinimidyl ester (Molecular Probes, Carlsbad, CA, USA) at its N-terminus. Pseudoproline dipeptide building blocks were purchased from NOVAbiochem. The incorporation of the pseudoproline building blocks into the sequence of the Vif CTD was performed essentially as described (Mutter *et al*., 1995) with the following modifications: The pseudoproline dipeptides were manually coupled in a manual SPPS vessel using a 2.5-fold excess of the pseudoproline in 8 ml NMP. A 2.5 eq. of HBTU were used as coupling agent, with 3 eq. of hydroxybenzotriazole (HOBt) and 6 eq. of DIEA. The protected pseudoproline was preactivated for 5 min prior to coupling at RT, and the coupling was performed overnight. Fmoc deprotection was performed with 20% piperidine in DMF for 20 min and was repeated twice. Kaiser test (Kaiser *et al*., 1970) and mass spectrometry analysis were performed after each step. All the peptides were purified as described (Katz *et al*., 2008).

Circular dichroism

Circular dichroism spectra were recorded using a J-810 spectropolarimeter (Jasco) in 25 mM potassium phosphate buffer, pH 7.3, 120 mM KCl and the following peptide concentrations: Vif CTD 51 μM and ElonginC 150 μM. The concentrations of both peptides in the 1:1 complex were 35 μM. All samples were measured in a 0.1 cm quartz cuvette for far-UV CD spectroscopy. Far-UV CD spectra were collected over a spectral range of 185–260 nm. Data were collected each 1 nm and averaged over 10 acquisitions. Prior to each experiment, the peptides were centrifuged at 13 200 rpm for 5 min and the UV spectrum between 200 and 400 nm was measured to calculate their concentration. Wavelength scans were corrected for buffer contributions and converted to molar ellipticity. Changes in the CD spectra were monitored as a function of temperature from 10 to 80°C with 10°C steps. Data were collected each 1 nm and averaged over five repeats. The molar ellipticity at 222 nm was fit to a linear model. The secondary structure content of Vif CTD with and without DPC was calculated using DichroWeb (Whitmore and Wallace, 2004) with the CDSSTR analysis algorithm.

Analytical gel filtration

Analytical gel filtration of purified $Vif_{141-192}$ at a concentration of 10 μM was performed on an ÄKTA Explorer (GE

Healthcare-Amersham Pharmacia, Giles, UK) using a Superose 30 analytical column 30 × 1 cm (GE Healthcare) equilibrated with buffer 20 mM Tris, pH 8, 0.1 M NaCl and 0.02% (w/v) sodium azide. The Vif CTD was eluted with a flow rate of 1 ml/min at 4°C, and the elution profile was recorded by continuously monitoring the UV absorbance at 220 nm. The calibration curve was made using molecular weight standards. The markers were: myoglobin, 17.0 kDa; RNaseA, 13.7 kDa; aprotinin, 6.5 kDa; and Vitamin B_{12}, 1.3 kDa.

Nuclear magnetic resonance

$Vif_{145-192}$ peptide in lyophilized form was dissolved in an aqueous solution (0.8 mM) of 25 mM potassium phosphate, 25 mM potassium chloride, 10% deuterium oxide (Aldrich) and 0.02% (w/v) sodium azide. The apparent pH was adjusted to 6.0 ± 0.2 with HCl and NaOH. The NMR experiments were performed at 20 ± 0.1°C on a Bruker Avance 600 MHz DMX spectrometer using standard TOCSY (Piotto *et al*., 1992) and ^{15}N-HSQC (Palmer *et al*., 1991) experiments. $^{3}J_{HNH\alpha}$ coupling values were fit to Lorentzian doublets using AURELIA (Bruker Analytische Messtechnik GmbH).

Binding studies using fluorescence spectroscopy

Measurements were performed at 10°C using a PerkinElmer LS-50b luminescence spectrofluorimeter equipped with a Hamilton microlabM dispenser as described in Hayouka *et al.* (2007). Peptide concentrations were determined using a UV spectrophotometer (Shimadzu, Kyoto, Japan). The fluorescein-labeled ElonginC_{76-111} peptide was dissolved in 25 mM potassium phosphate buffer, pH 6.8, ionic strength 150 mM. One milliliter of the labeled ElonginC_{76-111} solution was placed in a cuvette, and the non-labeled CTD of Vif (200 μl, 150 μM) was placed in the dispenser. Additions of 5 μl were titrated at 90 s intervals, the solution was stirred for 10 s and the fluorescence was measured after each addition using an excitation wavelength of 480 nm and an emission wavelength of 530 nm. Dissociation constants (K_d) were calculated by fitting the fluorescence titration curves (corrected for dilution) to a 1:1 binding model using KALEIDAGRAPH (Synergy Software, Reading, PA, USA). The following equation was used for the single-site model:

$$F = F_0 + \frac{\Delta F^*[\text{Vif CTD}]}{[\text{Vif CTD}] + K_d}$$

where F_0 is the initial fluorescence, ΔF is the amplitude of the fluorescence change from unbound and bound states, K_d is the dissociation constant, [Vif CTD] is the added concentration of Vif CTD peptides.

Disorder predictions

The sequence of the full length Vif (GeneBank code: AAZ14 773) was submitted to 11 publicly available servers, implementing 19 different algorithms for protein disorder prediction. In all cases, we used the default parameters. The methods are reviewed in Ferron *et al.* (2006).

Results

Synthesis of Vif CTD using pseudo-prolines

Our initial attempts to synthesize the Vif CTD by standard Fmoc chemistry resulted only in deleted and truncated peptides. Thus, Vif CTD peptides were synthesized using the pseudoproline building blocks method (Mutter *et al*., 1995), to avoid on-resin aggregation during the synthesis. The pseudoproline dipeptide substitution positions (residues 185, 179, 169 and 143; Fig. 1B) were located mainly at the C-terminus of the peptide. Using this method, we successfully synthesized the peptides. Synthesis of $Vif_{145-192}$ was more successful than the synthesis of the longer $Vif_{141-192}$ peptide, yielding higher amounts of pure peptide.

The CTD of Vif is natively unfolded under physiological conditions

The structural properties of free Vif CTD under physiological conditions were studied using several biophysical methods. The far-UV CD spectrum of the CTD (Fig. 2A) lacked the typical signatures of secondary structure, exhibiting only a negative signal at 200 nm. This pattern implied a high content of unstructured regions in the CTD. Changes in the signal at 222 nm as a function of temperature from 25 to 80°C showed a linear increase of ellipticity with increasing temperature (Fig. 2B). This increase indicated an apparent temperature-induced formation of residual (possibly helical) secondary structure, and was completely reversible. This set of CD spectra also revealed a well-defined iso-dichroic point at 212 nm, which may represent equilibrium among the unordered conformations and the induced conformation (Fig. 2B).

Analytical size-exclusion chromatography was used to analyze the degree of compactness of the CTD (Fig. 2C). The identities of all the peaks were verified by mass spectrometry. The CTD eluted from the column with an elution volume of 11.3 ml. This volume gave an apparent molecular weight of 14.0 kDa, a value 2.5 times higher than the calculated mass of 5.8 kDa according to the calibration curve of standard MW markers. This indicated an extended conformation of the Vif CTD.

The sequence of Vif was submitted to 11 publicly available servers for protein disorder prediction, which implement 19 algorithms (Fig. 3A). The algorithms chosen were based on different criteria to predict disordered conformations from sequences (reviewed in Ferron *et al*., 2006). In all cases we submitted the full-length Vif sequence (192 AA) and used the default parameters. All algorithms predicted disorder in the region of Vif CTD AA 151–192. AA 100–150 was predicted to have a folded conformation and the NTD 1–100 was controversial among the different servers (not shown). The CTD was analyzed for order/disorder promoting residues (Fig. 3B): 53.8% of the residues are disorder promoting (E, K, R, G, Q, S, P and A) and only 23.1% are order-promoting (I, L, V, W, F, Y and C). Furthermore, Vif CTD lacks any Phe or Cys residues that are known as order-promoting residues.

NMR of Vif CTD indicated an unstructured conformation

The ^{1}H-NMR spectra of $Vif_{145-192}$ showed a narrow dispersion of amide resonances, which is characteristic of a random coil (Fig. 4A). Methyl group residues gave resonances at 0.8 ppm (Val, Leu and Ile), 1.2 ppm (Thr) and

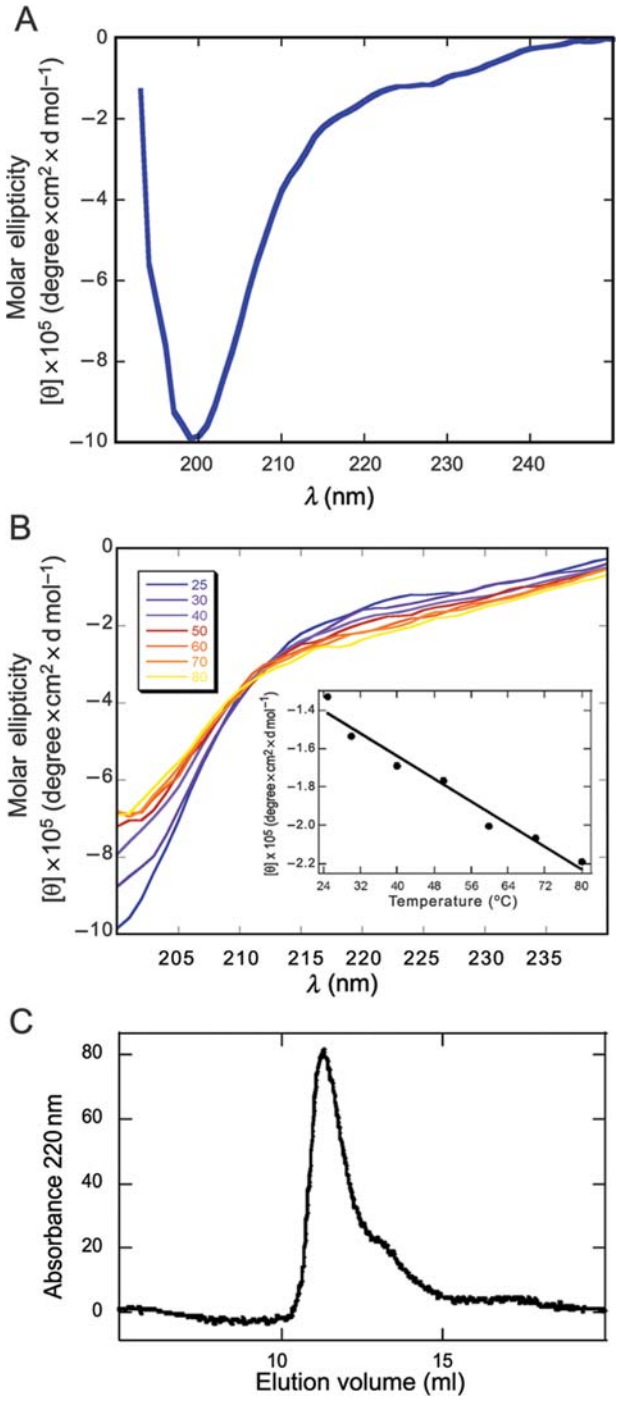

Fig. 2. Secondary structure analysis of Vif CTD: (**A**) Far-UV CD spectrum of Vif CTD in 25 mM phosphate buffer, pH 7.2 at 25°C and ionic strength of 150 mM. The strong absorption at 200 nm indicates that there are no α-helices or β-strands, giving the pattern of an unfolded peptide. (**B**) The effect of temperature on the CD spectrum of the CTD. All experiments were performed in 25 mM phosphate buffer, pH 7.2, ionic strength of 150 mM. The temperature range was 25–80°C. A linear increase in the CD signal at 222 nm as a function of temperature is consistent with an apparent temperature-induced formation of a residual structure that was completely reversible. (**C**) Analytical size exclusion chromatography of Vif CTD. The CTD was run on a Superdex 100 column. The elution volume of the CTD is 11.3 ml, which corresponds to a protein with MW of 14 kDa, which is ~2.5 times the calculated MW of 5.7 kDa.

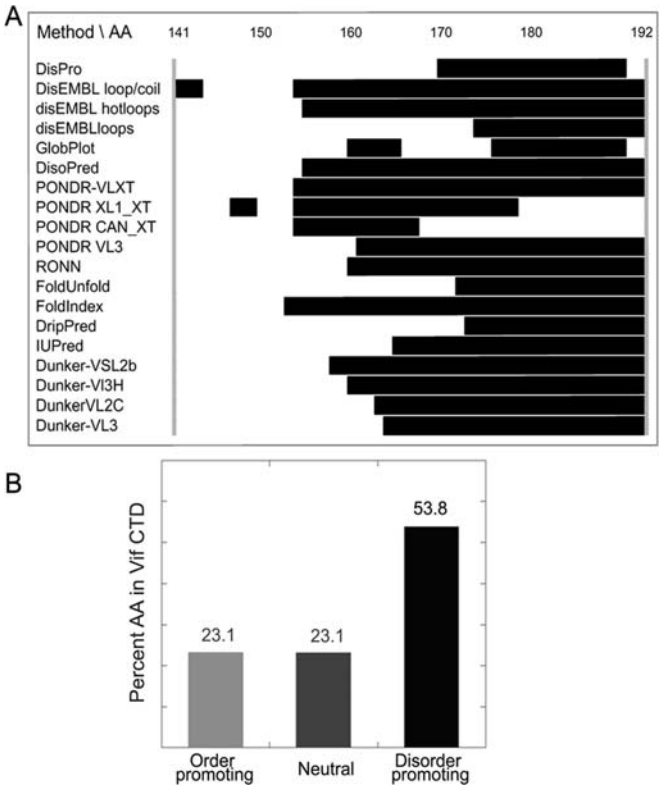

Fig. 3. Sequence analysis and disorder prediction of Vif CTD: (**A**) Disorder predictions for the Vif sequence were performed using 19 algorithms in publicly available servers. Each row depicts the disorder prediction of a different method on the Vif sequence. Segments that are predicted to be disordered are represented in black rectangles. Vif CTD 150–192 is predicted to be in an unfolded conformation. (**B**) Distribution of order- and disorder-promoting residues in the sequence of Vif CTD. The residues are classified as order promoting (I, L, V, W, F, Y and C), disorder promoting (E, K, R, G, Q, S, P and A) and neutral (all the others).

1.4 ppm (Ala), and were not shifted upfield, as would be expected for a structured protein. The dispersion of the amide protons in the ^{15}N-HSQC spectrum (Fig. 4B) was in a narrow range of 7.95–8.74 ppm, $\Delta = 0.79$ ppm, characteristic of unfolded proteins and peptides. $^{3}J_{\mathrm{HNH}\alpha}$ coupling constants, fit to rows from the TOCSY spectra, ranged between 5.1 and 7.5 Hz (three values were unresolved), indicating again an unstructured conformation (data not shown) (Dyson and Wright, 1998; Barbar, 1999; Dyson and Wright, 2004).

Vif CTD changed its conformation upon binding DPC micelles but not upon binding to ElonginC-derived peptide

Natively unfolded protein domains sometimes gain a defined structure upon ligand binding (Wright and Dyson, 1999; Dunker *et al.*, 2001). The structure of the Vif CTD bound to the ElonginBC complex shows the induction of helical structure in residues 145–153 (Stanley *et al.*, 2008). To test whether this is the case also for the Vif CTD, we examined whether its structure is affected by interacting with some of its natural binding partners: DPC micelles, as a model for the cell membrane, and a peptide derived from ElonginC. The CD spectrum of the CTD (Fig. 5A) in 5.4 mM DPC (green) and in 20 mM DPC (red), compared with the spectrum in buffer without DPC (blue), showed a red shift of ~3 nm (from 199 to 202 nm). The minimum at 198 nm decreased, while the signal at 222 nm increased. The change in the CD spectrum indicates a structural change in the Vif CTD that was induced by the micellar environment. We chose ElonginC as a model to study how peptide binding

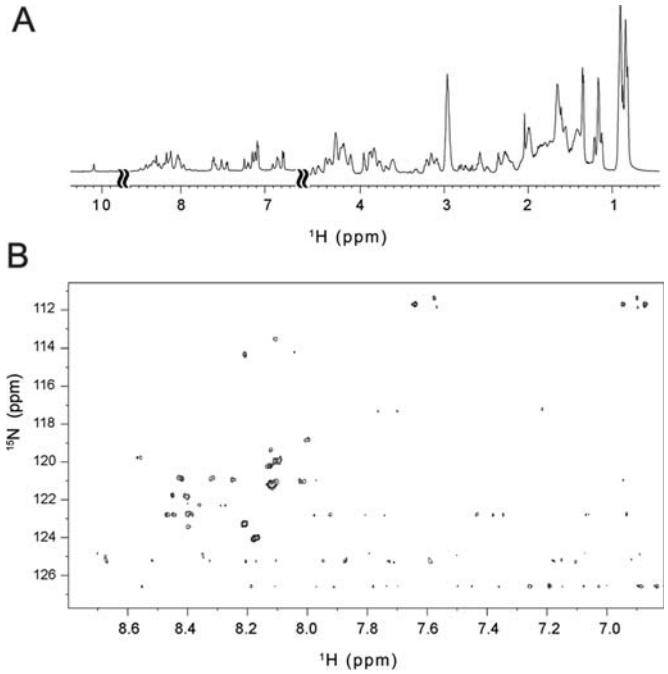

Fig. 4. Analysis of Vif CTD using NMR spectroscopy: (**A**) The ^{1}H-NMR spectrum of $Vif_{145-192}$ in 90% 25 mM phosphate buffer, 10% D_2O, pH 5 at 21°C, ionic strength of 150 mM and 0.02% NaN_3. The resonances are in general clustered, as expected for an unstructured peptide, and not dispersed as would be expected for a structured polypeptide. (**B**) The $^1H-^{15}N$ HSQC spectrum at natural abundance of $Vif_{145-192}$ reflecting the pattern of an unfolded protein. The spectrum was determined in 90% 25 mM phosphate buffer, 10% D_2O, pH 6 at 15°C, ionic strength 150 mM and 0.02% NaN_3. The fingerprint resonances range over 7.95–8.74 ppm, $\Delta = 0.79$ ppm.

affects the structure of the Vif CTD. The interaction between Vif CTD and the $ElonginC_{76-111}$ peptide, derived from the Vif binding region, was characterized using fluorescence spectroscopy and CD. $Vif_{141-192}$ was titrated into fluorescein-labeled $ElonginC_{76-111}$ and the resulting binding curve was fit to 1:1 binding model, resulting in K_d of 11.0 ± 0.6 μM (Fig. 5B). $Vif_{145-192}$ bound the ElonginC peptide with similar affinity, $K_d = 12.5 \pm 0.3$ μM. The CD spectrum of Vif CTD—$ElonginC_{76-111}$ mixture at 1:1 molar ratio (Fig. 5C) gave an average between the unbound spectra of the CTD and the free $ElonginC_{76-111}$, indicating that there is no significant change in the CTD structure upon binding to $ElonginC_{76-111}$ at this molar ratio.

Discussion

The current study provides direct evidence for the unfolded structure of the free CTD of Vif under physiological conditions using a variety of biophysical methods. Using peptides to study protein domains overcomes many obstacles of working with full-length proteins. In the case of the Vif protein, we used chemical synthesis to avoid the expression and purification problems that have hampered such studies so far. In our study, the Vif CTD-derived peptide was designed to represent a functionally independent domain and our results confirm its predicted unfolded nature.

The CTD of Vif is natively unfolded in its unbound state

The far-UV CD and NMR results indicated that the CTD is unfolded and lacks significant secondary structure elements

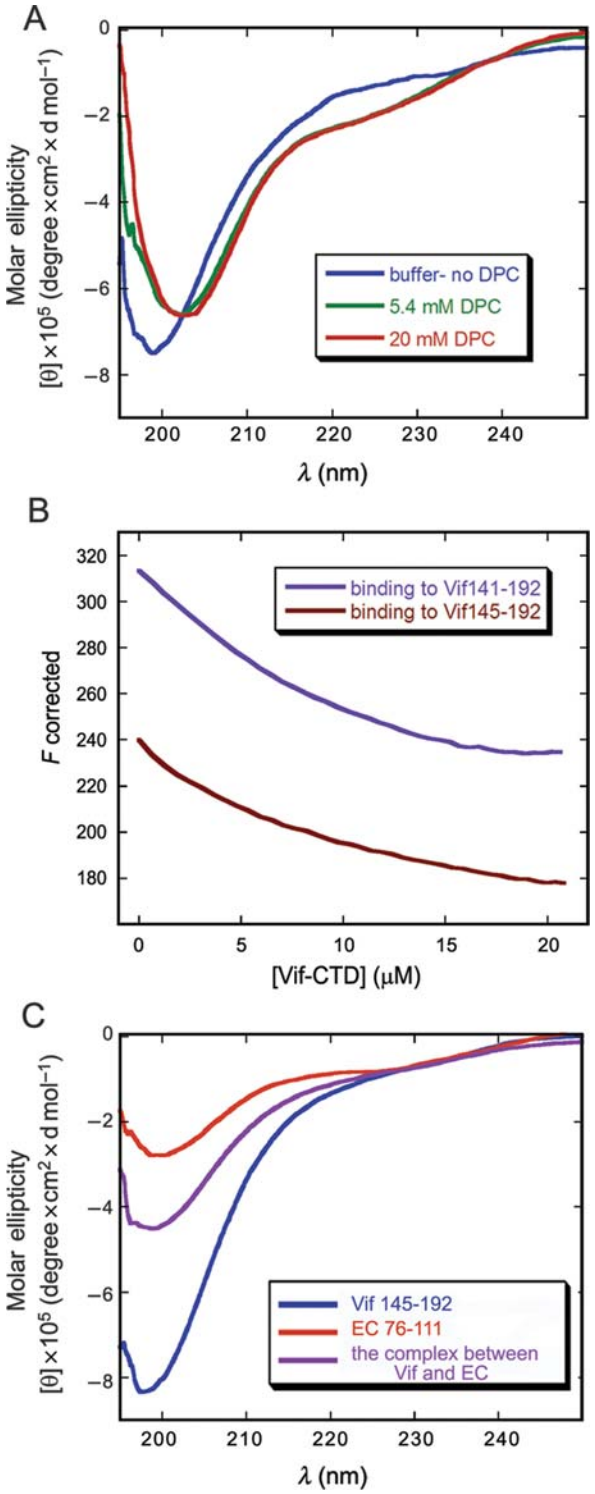

Fig. 5. Effect of ligand binding on Vif CTD structure: (**A**) The Vif $CTD_{145-192}$ CD spectrum changes upon adding DPC micelles. All the experiments were performed in 25 mM phosphate buffer, pH 7.2 at 25°C and an ionic strength of 150 mM without DPC (blue), with 5.4 mM DPC (green) or with 20 mM DPC (red). The signal at 198 nm decreases in DPC and the signal at 222 nm increases. There is also a red shift in the spectrum in the presence of DPC. (**B**) Binding of Vif CTD to $ElonginC_{76-111}$. Vif CTD peptides (200 μM) were titrated into the fluorescein-labelled $ElonginC_{76-111}$ peptides (100 nM). Both $Vif_{141-192}$ (purple) and $Vif_{145-192}$ (red) bind the Vif CTD with similar dissociation constants of 11 ± 0.6 and 12 ± 0.3 μM, respectively. (**C**) The CD spectrum of the complex between $Vif_{145-192}$ and $ElonginC_{76-111}$ (at 1:1 molar ratio) appears as an average (red) between the spectra of the free Vif CTD (blue) and $ElonginC_{76-111}$ (red), under the same conditions of 25 mM phosphate buffer, pH 7.2 at 25°C and an ionic strength of 150 mM.

under physiological conditions. The analytical size-exclusion chromatography showed that the CTD has a low level of compactness that confirmed an extended conformation, with high flexibility in the backbone. These results imply that Vif CTD has an effective conformation that is larger than that expected for a globular protein, typical of denatured or natively unfolded polypeptides. Sequence analysis revealed a majority of disorder promoting amino acids, and lack of order promoting residues such as cysteine and phenylalanine. Structure disorder predictions corroborated these findings, predicting an unfolded nature for AA 151–192. These results provide direct evidence of the unfolded nature of the free Vif CTD, in agreement with previous findings from modeling (Balaji *et al*., 2006) as well as cross-linking, proteolysis and mass spectrometry analyses (Auclair *et al*., 2007).

Implications of the conformational changes in the CTD

The increase in the CD signal at 222 with increasing temperature, as well as the iso-dichroic point that indicates a conformational equilibrium between the two states, imply that local elements of secondary structure may be induced in this region. Such residual structure is often displayed by intrinsically unstructured proteins (Uversky, 2002; Tompa, 2005) and may represent the basis for adopting a specific conformation at the CTD when binding to one of the partners of Vif or upon oligomerization. The pattern revealed by CD, upon changing the temperature, may result from an induced α-helix or left-handed polyproline type II-like (ppII) helix. We propose that the natively unfolded Vif CTD may contain residual structure in its unbound state. This serves as a starting point for the induction of helical structure upon interacting with binding partners.

The structure of Vif in complex with ElonginBC has revealed that residues 145–153 adopt a helical conformation in the bound state (Stanley *et al*., 2008), in agreement with two homology models based on the VHL-ElonginBC complex (Mehle *et al*., 2004; Yu *et al*., 2004) and with secondary structure predictions (Barraud *et al*., 2008) of this region. Binding of Vif CTD to a peptide derived from the Vif binding region in ElonginC did not cause the structural change expected from the crystal structure. This may be due to the following reason: A structural change upon interaction with a binding protein may require the presence of several different elements in the full-length binding partner. Binding of the CTD to the ElonginC peptide may be sufficient to form a complex, but not to promote the structural change in the CTD. Moreover, the helix conformation of residues 140–155 of Vif may be a result of the presence of both full-length ElonginC and ElonginB, or even by an indirect structural arrangement of the complete E3 ubiquitin ligase complex.

A moderate change in the conformation of the CTD is observed in DPC micelles. This may represent a change in the conformation of a portion of the CTD molecule in all of the molecules in solution or a change in a fraction of the molecules that are in direct contact with the DPC micelles. An analysis of the secondary structure content of Vif CTD with and without DPC using DichroWeb (Whitmore and Wallace, 2004) showed a decrease in the unordered fraction of the CTD from 60 to 38% and an increase in the β strand content from 13 to 38%. The Vif CTD has properties that may enable it to adopt a variety of conformations according to its binding partner.

DPC resembles common phosphatidylcholine lipids and forms micelles with a critical micelle concentration (CMC) of 1.2 mM, making it is a good model for the environment of the cell membrane. Different concentrations of DPC affect the phospholipid packing of the micelles (Tieleman *et al*., 2000). A sample of 20 mM DPC forms a more organized micellar environment than a sample of 5.4 mM DPC. However, in both cases, the DPC concentration is well above its CMC. Our results show a similar conformational change of the Vif CTD at both DPC concentrations, suggesting that the difference in the Vif CTD conformation is not related to the degree of compactness of the phospholipids in the DPC and thus maybe also in the host cell membrane. The DPC-induced conformational changes in the unstructured Vif domain may influence the ability of the CTD to interact with specific binding partners.

Helix conformations of the ppII type are common in unfolded regions (Rath *et al*., 2005). Peptides of poly-proline and poly-lysine have been shown to adopt ppII conformations (Rucker and Creamer, 2002). These residues are common in the Vif region P^{156}–S^{165} (**PKKI*K*PP*L*P*S***), suggesting that it may form a ppII substructure. Mutating the ^{161}PPLP^{164} conserved sequence has been shown to be crucial for Vif multimerization and eliminated Vif activity (Simon *et al*., 1999). A conformational change that results in a ppII structure may be part of some control mechanism through multimerization. Ser165, which is located at the end of this motif, is known to be phosphorylated (Yang and Gabuzda, 1998). Such phosphorylation may induce a structural change that takes part in this control mechanism. These structural elements in the CTD may form initial contacts with different interaction partners, which induce folding in the unstructured polypeptide according to the binding region of the specific partner that serves as a template for CTD folding.

Biological implications

The unfolded nature of the Vif CTD may enable binding different partner molecules through the same region, as is typical for natively unfolded proteins (Fink, 2005). Disordered regions have a higher frequency of known phosphorylation sites than ordered regions (Iakoucheva *et al*., 2004). The CTD of Vif is phosphorylated by MAPK at Ser144, Thr155, Ser165 and Thr188 (Yang *et al*., 1996). Reversible phosphorylation represents an important regulatory mechanism and conformational changes upon phosphorylation are well known and often affect protein function. Hence, the CTD may have a regulatory role, maintained by its phosphorylation state, as suggested above for Ser165. This is further supported by the observation that the CTD of Vif is processed by the viral protease, between AA 150–151, releasing the CTD as a 42-residue polypeptide (Khan *et al*., 2002). This could remove the regulation imposed by the CTD. This cleavage of Vif indicates that the C-terminal Vif peptide may have biological roles of its own, making peptides a relevant model for the Vif CTD in our case since they also represent a complete biologically active domain.

The CTD of Vif binds many target proteins, suggesting that it plays an important role in the function of Vif during HIV infection. The unfolded state of the CTD, which

enables it to adopt different structural conformations induced by different partner molecules, may be a mechanism of maximizing the efficiency of this protein. Characterizing the interactions mediated through the CTD and their relation to the unfolded state of the CTD will be crucial for fully understanding the mechanism of action of Vif and may be used for rational design of Vif inhibitors to serve as anti-HIV lead compounds.

Acknowledgements

We thank Prof. Moshe Kotler for his help.

Funding

This work was supported by the Israeli Ministry of Health and by the US–Israel Binational Science Foundation (BSF). T.H.R. was partly supported by the ISEF Foundation. H. B. was supported by a post-doctoral fellowship from the Lady Davis Fellowship Trust.

References

Auclair,J.R., Green,K.M., Shandilya,S., Evans,J.E., Somasundaran,M. and Schiffer,C.A. (2007) *Proteins*, **69**, 270–284.
Balaji,S., Kalpana,R. and Shapshak,P. (2006) *Bioinformation*, **1**, 290–309.
Barbar,E. (1999) *Biopolymers*, **51**, 191–207.
Barraud,P., Paillart,J.C., Marquet,R. and Tisne,C. (2008) *Curr. HIV Res.*, **6**, 91–99.
Borman,A.M., Quillent,C., Charneau,P., Dauguet,C. and Clavel,F. (1995) *J. Virol.*, **69**, 2058–2067.
Bouyac,M.M., *et al*. (1997) *J. Virol.*, **71**, 9358–9365.
Cao,J., Isaacson,J., Patick,A.K. and Blair,W.S. (2005) *Antimicrob. Agents Chemother.*, **49**, 3833–3841.
Dunker,A.K.J.D., *et al*. (2001) *J. Mol. Graph. Model*, **19**, 26–59.
Dyson,H.J. and Wright,P.E. (1998) *Nat. Struct. Biol.*, **5**(Suppl.), 499–503.
Dyson,H.J. and Wright,P.E. (2004) *Chem. Rev.*, **104**, 3607–3622.
Dyson,H.J. and Wright,P.E. (2005) *Nat. Rev. Mol. Cell Biol.*, **6**, 197–208.
Ferron,F., Longhi,S., Canard,B. and Karlin,D. (2006) *Proteins*, **65**, 1–14.
Fink,A.L. (2005) *Curr. Opin. Struct. Biol.*, **15**, 35–41.
Goncalves,J., Jallepalli,P. and Gabuzda,D.H. (1994) *J. Virol.*, **68**, 704–712.
Goncalves,J., Shi,B., Yang,X. and Gabuzda,D. (1995) *J. Virol.*, **69**, 7196–7204.
Hayouka,Z., Rosenbluh,J., Levin,A., Loya,S., Lebendiker,M., Veprintsev,D., Kotler,M., Hizi,A., Loyter,A. and Friedler,A. (2007) *Proc. Natl. Acad. Sci. USA*, **104**, 8316–8321.
Iakoucheva,L.M., Radivojac,P., Brown,C.J., O'Connor,T.R., Obradovic,Z. and Dunker,A.K. (2004) *Nucleic Acids Res.*, **32**, 1037–1049.
Kaiser,E., Colescott,R.L., Bossinger,C.D. and Cook,P.I. (1970) *Anal. Biochem.*, **34**, 595–598.
Katz,C., *et al*. (2008) *Proc. Natl. Acad. Sci. USA*, **105**, 12277–12282.
Khan,M.A., Akari,H., Kao,S., Aberham,C., Davis,D., Buckler-White,A. and Strebel,K. (2002) *J. Virol.*, **76**, 9112–9123.
Lake,J.A., Carr,J., Feng,F., Mundy,L., Burrell,C. and Li,P. (2003) *J. Clin. Virol.*, **26**, 143–152.
Lv,W., Liu,Z., Jin,H., Yu,X., Zhang,L. and Zhang,L. (2007) *Org. Biomol. Chem.*, **5**, 617–626.
Mariani,R., Chen,D., Schrofelbauer,B., Navarro,F., Konig,R., Bollman,B., Munk,C., Nymark-McMahon,H. and Landau,N.R. (2003) *Cell*, **114**, 21–31.
Mehle,A., Goncalves,J., McPike,M. and Gabuzda,D. (2004) *Genes Dev.*, **18**, 2861–2866.
Mutter,M., Nefzi,A., Sato,T., Sun,X., Wahl,F. and Wohr,T. (1995) *Pept. Res.*, **8**, 145–153.
Palmer,A.G., III, Cavanagh,J., Wright,P.E. and Rance,M. (1991) *J. Magn. Reson.*, **93**, 151–170.
Piotto,M., Saudek,V. and Sklenar,V. (1992) *J. Biomol. NMR*, **2**, 661–665.
Rath,A., Davidson,A.R. and Deber,C.M. (2005) *Biopolymers*, **80**, 179–185.
Rucker,A.L. and Creamer,T.P. (2002) *Protein Sci.*, **11**, 980–985.
Simon,J.H., Fouchier,R.A., Southerling,T.E., Guerra,C.B., Grant,C.K. and Malim,M.H. (1997) *J. Virol.*, **71**, 5259–5267.
Simon,J.H., Sheehy,A.M., Carpenter,E.A., Fouchier,R.A. and Malim,M.H. (1999) *J. Virol.*, **73**, 2675–2681.
Sodroski,J., Goh,M.H., Tartar,A., Portetelle,D., Burny,A. and Haseltine,W. (1986) *Science*, **231**, 1549–1553.
Stanley,B.J., Ehrlich,E.S., Yu,Y., Xiao,Z., Yu,X.F. and Xiong,Y. (2008) *J. Virol.*, **82**, 8656–8663.
Strebel,K., Daugherty,D., Clouse,K., Cohen,D., Folks,T. and Martin,M.A. (1987) *Nature*, **328**, 728–730.
Tieleman,D.P., van der Spoel,D. and Berendsen,H.J.C. (2000) *J. Phys. Chem. B*, **104**, 6380–6388.
Tompa,P. (2002) *Trends Biochem. Sci.*, **27**, 527–533.
Tompa,P. (2005) *FEBS Lett.*, **579**, 3346–3354.
Uversky,V.N. (2002) *Protein Sci.*, **11**, 739–756.
Uversky,V.N., Gillespie,J.R. and Fink,A.L. (2000) *Proteins*, **41**, 415–427.
Whitmore,L. and Wallace,B.A. (2004) *Nucleic Acids Res.*, **32**, W668–W673.
Wright,P.E. and Dyson,H.J. (1999) *J. Mol. Biol.*, **293**, 321–331.
Yang,X. and Gabuzda,D. (1998) *J. Biol. Chem.*, **273**, 29879–29887.
Yang,X., Goncalves,J. and Gabuzda,D. (1996) *J. Biol. Chem.*, **271**, 10121–10129.
Yang,S., Sun,Y. and Zhang,H. (2001) *J. Biol. Chem.*, **276**, 4889–4893.
Yang,B., Gao,L., Li,L., Lu,Z., Fan,X., Patel,C.A., Pomerantz,R.J., DuBois,G.C. and Zhang,H. (2003) *J. Biol. Chem.*, **278**, 6596–6602.
Yu,X., Yu,Y., Liu,B., Luo,K., Kong,W., Mao,P. and Yu,X.F. (2003) *Science*, **302**, 1056–1060.
Yu,Y., Xiao,Z., Ehrlich,E.S., Yu,X. and Yu,X.F. (2004) *Genes Dev.*, **18**, 2867–2872.

Received January 7, 2009; revised January 7, 2009; accepted January 15, 2009

Edited by Gideon Schreiber, Board Member for PEDS.